NASA TECHNICAL NOTE

NASA TN D-6044

LONG TIME CREEP BEHAVIOR OF TANTALUM - 10 TUNGSTEN IN HIGH VACUUM

by Robert H. Titran and William D. Klopp

Lewis Research Center
Cleveland, Ohio 44135

NATIONAL AERONAUTICS AND SPACE ADMINISTRATION • WASHINGTON, D. C. • OCTOBER 1970

1. Report No. NASA TN D-6044	2. Government Accession No.	3. Recipient's Catalog No.
4. Title and Subtitle LONG TIME CREEP BEHAVIOR OF TANTALUM - 10 TUNGSTEN IN HIGH VACUUM		5. Report Date October 1970
		6. Performing Organization Code
7. Author(s) Robert H. Titran and William D. Klopp		8. Performing Organization Report No. E-5389
9. Performing Organization Name and Address Lewis Research Center National Aeronautics and Space Administration Cleveland, Ohio 44135		10. Work Unit No. 129-03
		11. Contract or Grant No.
12. Sponsoring Agency Name and Address National Aeronautics and Space Administration Washington, D.C. 20546		13. Type of Report and Period Covered Technical Note
		14. Sponsoring Agency Code

15. Supplementary Notes

16. Abstract

The high vacuum creep behavior of tantalum - 10 tungsten in the 2000° to 2600° F (1093° to 1426° C) range was studied for times up to 10 000 hours. The creep strength was found to be related to grain size, the secondary creep rate increasing with decreasing grain size. The exponential factor n relating creep rate to applied stress was found to increase with increasing grain diameter. Analysis of the creep curves showed that after an initial period of decreasing creep rate, the creep rate gradually increased with time. Creep strain during the nonlinear second-stage creep was proportional to time$^{3/2}$.

17. Key Words (Suggested by Author(s)) Tantalum alloy; creep; grain size; temperature dependency - (activation energy); stress dependency; high vacuum; grain boundary sliding; secondary creep; deformation mechanism; dislocation climb

18. Distribution Statement Unclassified - unlimited

19. Security Classif. (of this report)	20. Security Classif. (of this page)	21. No. of Pages	22. Price *
Unclassified	Unclassified	22	$3.00

*For sale by the Clearinghouse for Federal Scientific and Technical Information Springfield, Virginia 22151

LONG TIME CREEP BEHAVIOR OF TANTALUM - 10 TUNGSTEN IN HIGH VACUUM

by Robert H. Titran and William D. Klopp

Lewis Research Center

SUMMARY

A study was made of the long-time, high vacuum creep behavior of polycrystalline 90 tantalum - 10 tungsten (Ta-10W) sheet at temperatures near one-half the melting point. The creep curves were unusual in that the secondary creep rate increased with time under constant load, beginning at total strains less than 0.2 percent. It was determined that creep strain was proportional to time$^{3/2}$ during this second-stage creep. This is believed to result from a concurrent diffusion controlled reaction, such as desegregation of tungsten from grain boundary regions.

The predominant deformation mechanism of Ta-10W under the imposed test conditions is attributed to grain boundary sliding. However, the activation energy for creep suggests that deformation by dislocation climb in regions adjacent to the grain boundaries, which accommodates grain boundary sliding, may be rate controlling.

Grain size exerts a significant effect on creep behavior. The creep strength decreases with decreasing grain size. Creep rate ϵ/t was related to applied stress σ_a, grain size L, and temperature T by

$$\frac{\epsilon^{2/3}}{t} = \dot{\beta} = K\left(\sigma_a + \frac{A}{L^2}\right)^{n'} e^{-Q_c/RT}$$

where

$$K = 8.35\times10^{-10}\ \text{sec}^{-1}\ (\text{psi})^{-3.47}$$

$$A = 0.0389\ \text{psi}\ (\text{cm})^2$$

$$n' = 3.47$$

$$Q_c = 90\ 400\ \text{cal/g-mole}$$

$$R = 1.986\ \text{cal/g-mole}$$

INTRODUCTION

Several tantalum alloys are currently of interest as containment materials for liquid alkali metals in advanced space power systems. These alloys include T-111 (Ta-8W-2Hf), T-222 (Ta-9.6W-2.4Hf-0.01C), and ASTAR-811C (Ta-8W-1Re-1Hf-0.015C), all of which possess adequate resistance to liquid metal corrosion and good creep strength for the intended application. These space power systems are intended to operate for long times, 10 000 to 50 000 hours, at temperatures in the 2000° to 2600° F (1093° to 1426° C) range.

During previous long-time creep evaluation of these and other candidate alloys of tantalum and of columbium (refs. 1 to 6), several features of the creep behavior were observed which merited further attention. These features were, first, a strong dependence of creep rate on grain size, with coarse grained materials exhibiting lower creep rates than fine grained materials, and second, a continually increasing second-stage creep rate at strains under 1 percent at constant load and constant temperature.

The effects of grain size on creep rate have received increasing attention during the past decade. The concept advanced by Garofalo (ref. 7) appears to be qualitatively applicable to many metals and alloys and states the following:

(1) At low temperatures (or high $\dot{\epsilon}/D$), Petch-type strengthening occurs, with fine-grained materials being stronger.

(2) At intermediate temperatures, the highest creep strength is observed at an optimum intermediate grain size.

(3) At high temperatures (or low $\dot{\epsilon}/D$), grain boundary sliding predominates, and coarse-grained materials are strongest.

Garofalo has further suggested that grain size effects on creep can be expressed as

$$\dot{\epsilon} = K\left(\frac{2L_m^3 + L^3}{L}\right)(\sinh \alpha\sigma)^n e^{-Q/RT} \tag{1}$$

where L is the grain diameter and L_m is the grain diameter observed at the minimum for secondary creep rate.

One effect of alloying is apparently to lower the temperature at which grain boundary sliding predominates over grain boundary strengthening, so that coarse-grained alloys generally have higher creep strength than fine-grained alloys. However, the improved creep strength associated with higher pretest annealing temperatures observed for Cb-1Zr (ref. 4) and FS-85 (Cb-27Ta-10W-1Zr) (ref. 5) have been ascribed to changes in precipitate morphology rather than to grain size effects on creep mechanism.

The increasing creep rate at low strains observed during long-time creep of many columbium and tantalum alloys contrasts sharply with the intermediate period of linear

creep normally observed for pure metals and many alloys at temperatures near 0.5 T_m. However, there have been other observations of unusual creep curves. For example, Lawley, Coll, and Cahn (ref. 8) have observed accelerating creep in polycrystalline iron-aluminum alloys tested near the order-disorder transformation temperature which they attribute to stress-induced short-range directional ordering. Howard et al. (ref. 9) have also observed brief initial accelerating creep in single crystals of silver - aluminum, attributed to localized stress-induced disordering near dislocations. In contrast to the previous mechanisms involving stress-induced diffusion, Sheffler et al. (ref. 6) have suggested that the increasing creep rates in the tantalum alloy T-111 are a result of oxygen loss during high-vacuum testing which reduces strain aging and cause progressive weakening of the alloy. In view of the fact that the phenomenon has been observed for extended time periods during the creep of tantalum and columbium alloys of various composition and under varying vacuum conditions (some of which resulted in oxygen pick up rather than loss), it seemed desirable to further investigate this phenomenon.

The purpose of the present investigation was to better define the long-time creep behavior of tantalum alloys with particular respect to the effects of grain size on creep rate and the accelerating creep rates. In order to eliminate the complicating effects of carbide or oxide precipitates, the single phase solid-solution alloy Ta-10W was chosen for study, with the expectation that results on this material would be at least partially applicable to the more complex Ta-W-(Hf-HfC) base alloys. Tests were conducted at stresses from 6000 to 15 900 psi (41.37 to 109.63 MN/m^2) in the temperature range 2000^o to 2462^o F (1093^o to 1350^o C) to approximate expected service conditions in future space power systems.

SYMBOLS

A, B, K, α	constants
a, b, c, d	coefficients of polynomials
C	circumference of circle, cm
D	diffusion coefficient, $(cm^2)(sec^{-1})$
L	average grain diameter, cm
L_m	average grain diameter at minimum secondary creep rate, cm
M	projected magnification, diam
N	number of grain boundary intercepts
n	exponential dependency of creep rate on applied stress, σ_a

n' exponential dependency of creep rate on effective stress, σ_e

Q_c apparent activation energy for creep, cal/g-mole

Q_d activation energy for diffusion, cal/g-mole

R gas constant, 1.986 cal/g-mole

T absolute temperature, K

t time, sec

$\dot{\alpha}$ primary creep rate constant, $(\text{strain}^2)(\text{sec}^{-1})$

$\dot{\beta}$ secondary creep rate constant, $(\text{strain}^{2/3})(\text{sec}^{-1})$

ϵ creep strain

ϵ_o initial creep strain on loading

$\dot{\epsilon}_s$ secondary creep rate, sec^{-1}

σ_a applied stress, psi (MN/m^2)

σ_e effective stress, psi (MN/m^2)

MATERIAL AND PROCEDURES

The material used in this study was a 30-mil- (0.076-cm-) thick Ta-10W sheet procured commercially in the cold-worked condition. The manufacturer reported that the material had been cold-rolled 90 percent following the last in-process stress relief heat treatment. Chemical analysis of the sheet is shown in table I.

Creep specimens with a 1-inch (2.54-cm) gage length and a 0.250-inch (0.635-cm) gage width, as shown in figure 1, were machined from the sheet with the specimen axis parallel to the final rolling direction. These specimens were degreased in acetone, wrapped in clean tantalum foil, and then annealed for 1 hour in a titanium sputter ion pumped furnace at a vacuum of 10^{-7} torr at 2600°, 2800°, 3000°, 3200°, and 3600° F (1426°, 1537°, 1648°, 1759°, and 1982° C, respectively). Temperatures were measured

TABLE I. - CHEMICAL ANALYSIS OF TANTALUM - 10 TUNGSTEN SHEET

Element	Tungsten	Oxygen	Nitrogen	Carbon	Hydrogen	Tantalum
Composition, weight percent	10.35	0.0021	0.0040	0.0015	0.0001	Balance

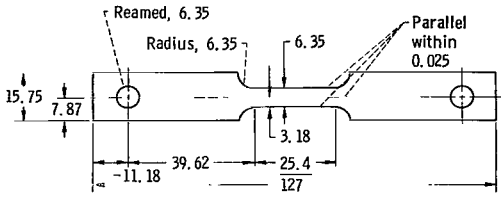

Figure 1. - Standard sheet creep-test specimen. (All dimensions are in millimeters.)

with a tungsten/tungsten - 26 percent rhenium thermocouple and are estimated to be accurate within 9° F (5° C).

All creep specimens were weighed to the nearest 0.1 milligram before and after annealing to determine if contamination resulted during heat treatment. In all cases, no significant weight changes were observed, indicating that the possible contamination amounted to a maximum of less than 10 ppm by weight.

These annealing schedules resulted in specimens with initial average grain diameters of 0.0022, 0.0026, 0.0035, 0.0053, and 0.0237 centimeter, respectively. Micrographs of representative structures after annealing are shown in figure 2. Grain sizes

(a) Temperature, 2800° F (1537° C).

(b) Temperature, 3000° F (1648° C).

Figure 2. - Structure of Ta-10W after annealing for 1 hour at indicated temperature. X250.

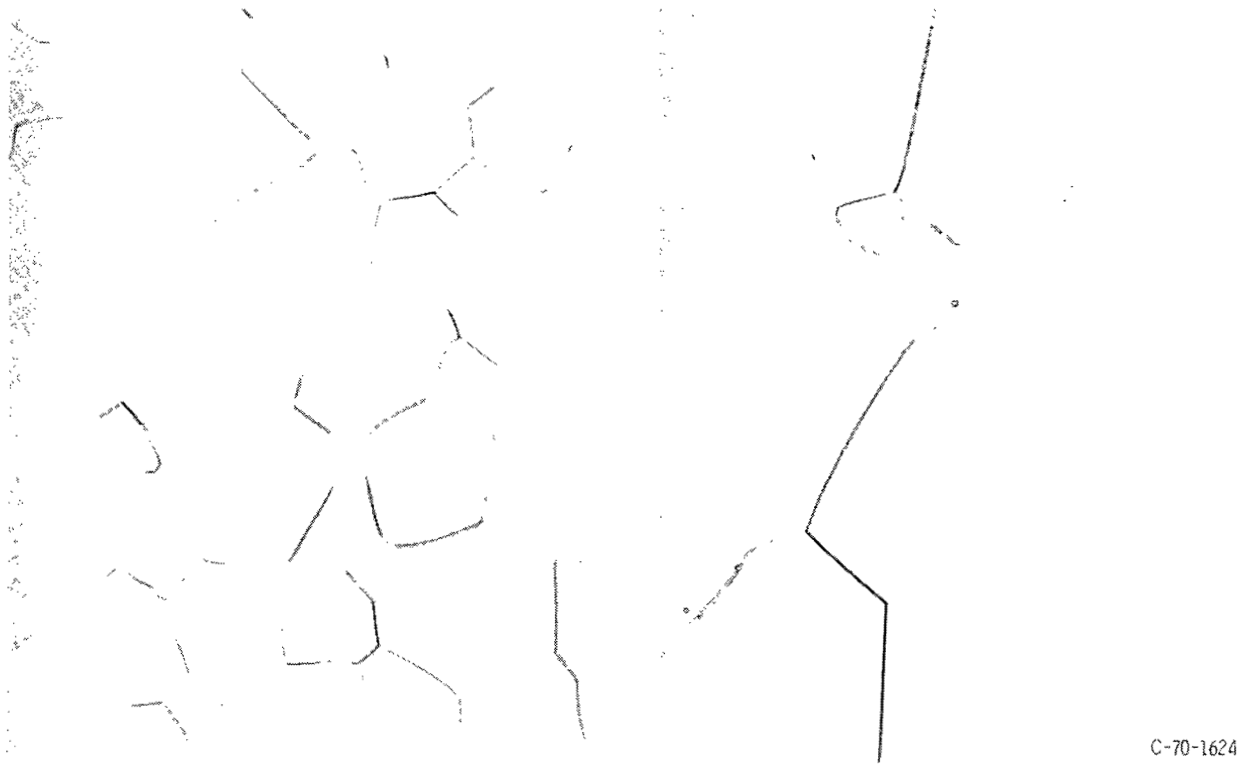

C-70-1624

(c) Temperature, 3200° F (1759° C).

(d) Temperature, 3600° F (1982° C).

Figure 2. - Concluded.

were also determined after creep testing; these final grain sizes were used in correlating grain sizes effects. The average grain diameters were determined by counting the number of boundary intercepts with a measured circle on a projection screen. The following relation was employed in calculating the grain diameter:

$$L = \frac{C}{MN}$$

where

L average grain diameter, cm

C circumference of circle, cm

M projected magnification

N number of grain boundary intercepts

At least ten counts were averaged for each specimen by two independent observers.

The titanium-sputter ion pumped, high-vacuum (10^{-9} torr) creep facilities used in this study are described in detail in reference 10. Creep strain measurements were performed optically. A cathetometer clamped to the furnace chamber frame was used to sight on Knoop hardness impressions placed 1.0 inch (2.54 cm) apart on the specimen. The precision of creep - strain measurements is estimated to be ±0.02 percent for the gage length used. In all instances, an initial gage length was read at the test temperature prior to the loading of the specimen. The strain on loading was measured and is incorporated in the reported total creep strain. Generally, this initial strain was less than 0.05 percent. Creep testing was usually terminated after a total creep strain of 2 to 3 percent.

Post-test examination included chemical analysis for possible oxygen contamination during testing, metallographic examination for grain size, etch pit formation, void and/or crack formation, and microhardness and X-ray microprobe analysis for possible solute segregation.

RESULTS AND DISCUSSION

Shape of Creep Curves

Typical creep curves for polycrystalline Ta-10W tested at 2372° F (1300° C), 2462° F (1350° C), and 6000 psi (41.37 MN/m^2) are shown in figure 3. These curves consist of a strain on loading (ϵ_o) of about 0.05 percent, a very short period of primary creep, and a secondary period of accelerating creep rate. There is no tertiary creep period due to the small strains over which these measurements were taken, usually about 2 percent. It is apparent from figure 3 that increasing the grain size from 0.0031 to 0.0053 centimeter substantially reduces the secondary creep rate.

Several techniques were utilized to determine the time dependency of the secondary creep period. The creep curves were analyzed by the geometric progression method of deLacombe as described by Crussard (ref. 11) and were also replotted against time$^{4/3}$ and time$^{3/2}$. Computer fittings to polynomials of the form

$$\epsilon - \epsilon_o = at + bt^2 + ct^3 \tag{2}$$

and

$$\epsilon - \epsilon_o = at^{1/2} + bt + ct^{3/2} \tag{3}$$

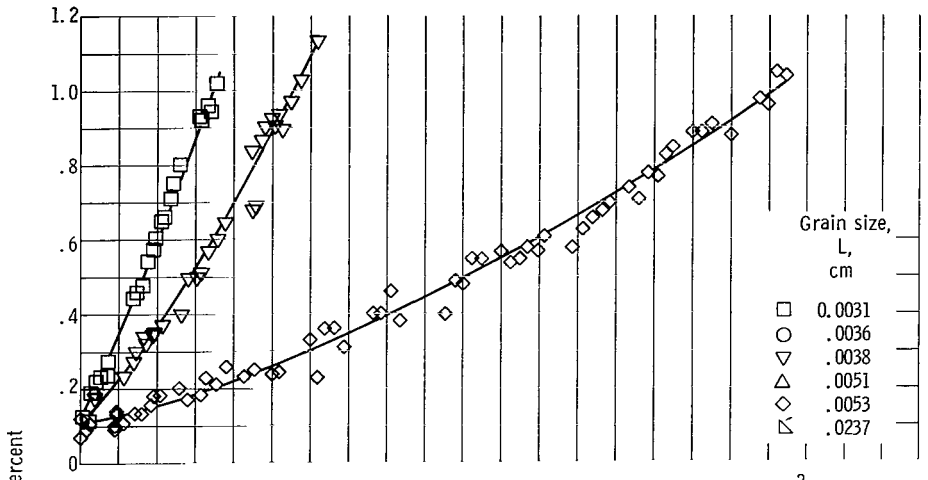

(a) Ta-10W creep curves at 2372° F (1300° C) and 6000 psi (41.37 MN/m^2).

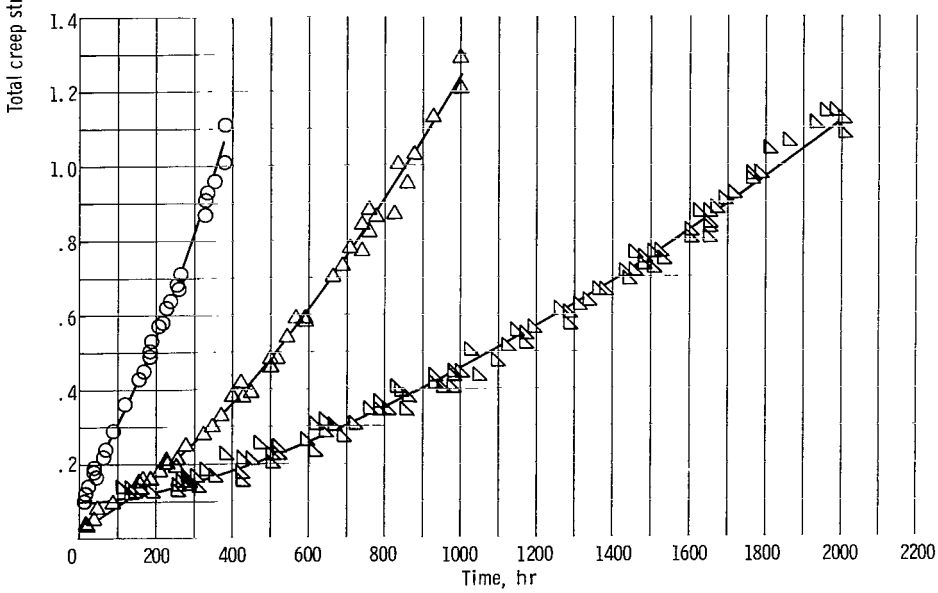

(b) Ta-10W creep curves at 2462° F (1350° C) and 6000 psi (41.37 MN/m^2).

Figure 3. - Effects of grain size on creep behavior of Ta-10W. Note upward concavity of creep curves which represents best fit of data to polynomial ($\epsilon = \epsilon_0 + at^{1/2} + bt^{3/2}$).

were also explored. These analyses indicated that the creep curves could be well described by a time$^{1/2}$ term during primary creep and a time$^{3/2}$ term during secondary creep. Since there was no apparent period of linear creep, the t term was dropped and all curves were computer fitted to the polynomial

$$\epsilon - \epsilon_o = at^{1/2} + bt^{3/2} \tag{4}$$

This relation was employed to obtain the smooth curves shown in figure 3.

Figure 4 illustrates the linearity of the strain-time curves when plotted against time$^{3/2}$, while figure 5 shows the computer-calculated instantaneous creep rates as functions of time. The simultaneous occurrence of the minimum creep rates shown in figure 5 indicates that the shapes of the creep curves are independent of the actual rates.

Creep rates for primary and secondary creep were determined from the strain-time coefficients of equation (4) by expressing a and b in terms of reciprocal time. The primary creep rate constant $\dot{\alpha}$ thus has units of (strain^2)(time^{-1}) and is equivalent to a^2, while the secondary creep rate constant $\dot{\beta}$ has units of (strain$^{2/3}$)(time^{-1}) and is equivalent to $b^{2/3}$. These rate constants are given in table II along with other details of the creep tests.

The uniform applicability of the time$^{3/2}$ function for secondary creep to the creep curves generated in this study strongly implies that accelerating creep is a basic feature of the test results rather than an extraneous feature such as a gross compositional change of the specimens during test. We suggest that the upward concavity of the creep

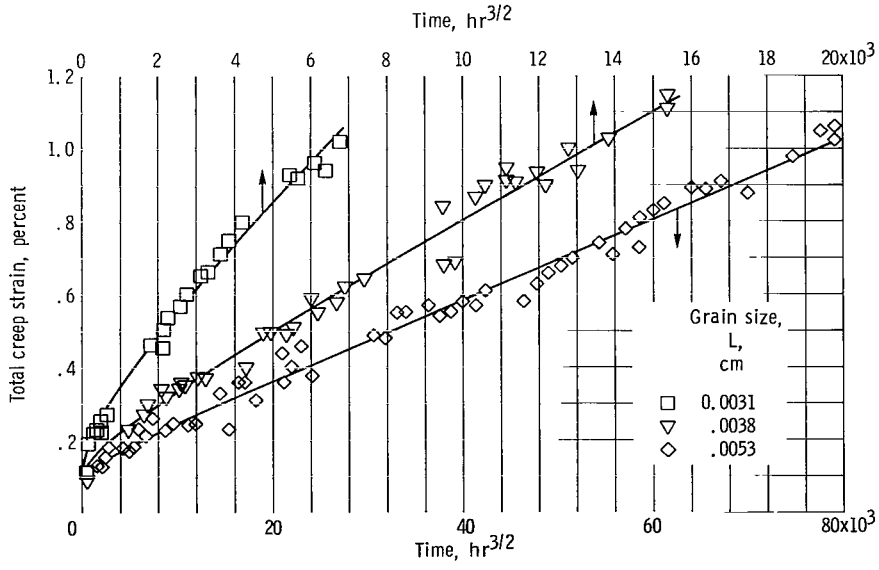

Figure 4. - Creep curves from figure 3(a) replotted against time$^{3/2}$. Note linearity at extended times.

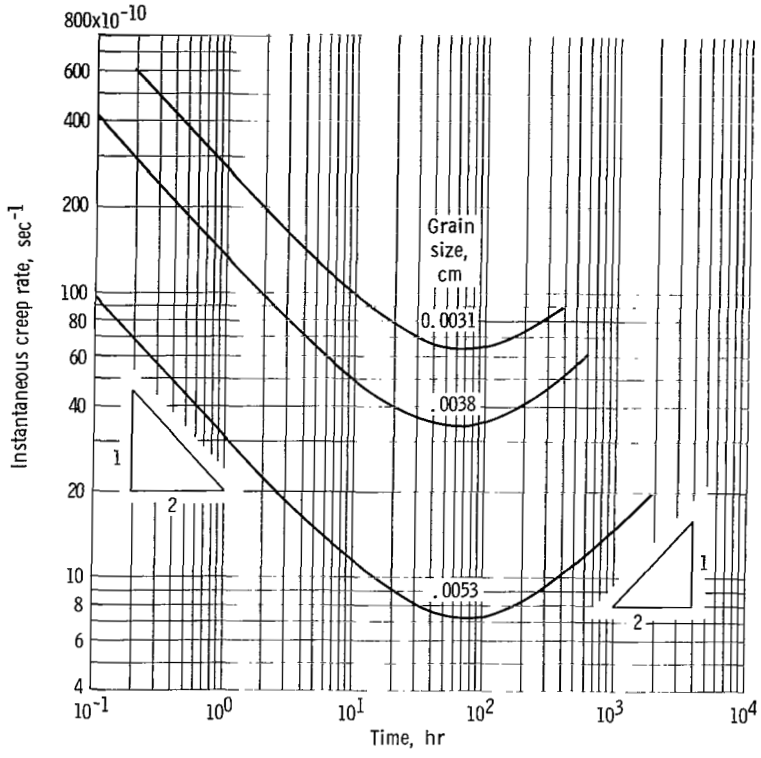

Figure 5. - Creep rate for curves shown in figure 3(a) calculated from best fits to polynomial ($\epsilon = \epsilon_0 + at^{1/2} + bt^{3/2}$). Note simultaneous occurrence of minimum creep rates.

curves results from a localized diffusion controlled reaction which occurs during creep and has a weakening effect on the specimen. The effect of such a reaction on secondary creep would be of the form

$$\epsilon - \epsilon_o = \dot{\epsilon} t(1 + kt)^{1/2} \tag{5}$$

where k reflects both the extent and rate of the diffusion reaction at constant temperature. It is easily seen that when $kt >> 1$, equation (5) reduces to

$$\epsilon - \epsilon_o = \dot{\epsilon} k^{1/2} t^{3/2} \tag{6}$$

giving the time$^{3/2}$ function for secondary creep deduced experimentally with $\dot{\epsilon} k^{1/2}$ equal to b in equation (4) and $\dot{\epsilon}^{2/3} k^{1/3}$ equal to $\dot{\beta}$ in table II. Unfortunately, it was not possible to separate $\dot{\beta}$ into creep and diffusion rate components.

TABLE II. - CREEP RATES AND STRAINS FOR POLYCRYSTALLINE 90Ta-10W SHEET

Specimen	1-Hour annealing temperature		Creep test temperature		Applied creep stress		Primary creep rate constant, $\dot{\alpha}$, $(\text{strain}^2)(\text{sec}^{-1})$	Time to reach minimum creep rate, hr	Secondary creep rate constant, $\dot{\beta}$, $(\text{strain}^{2/3})(\text{sec}^{-1})$	Time at temperature and load, hr	Strain achieved at temperature and load, percent	Average grain diameter, cm (a)		Hardness (10 kg VHN)		Oxygen pickup during testing, ppm
	°F	°C	°F	°C	psi	MN/m^2						Before creep testing	After creep testing	Before creep testing	After creep testing	
Constant temperature; constant load																
2	2600	1426	2200	1204	8 000	55.16	4.41×10^{-12}	200	0.981×10^{-8}	1006.6	1.13	0.0022	0.0024	223	214	12
3	3200	1759	2200	1204	12 000	82.74	.887	147	.706	1699.6	1.15	-----	.0044	199	222	158
4	2600	1426	2000	1093	15 900	109.63	14.6	---	----	1341.1	1.07	.0022	.0022	180	211	24
5	3600	1982	2200	1204	12 000	82.74	.304	244	.352	3018.3	1.12	-----	.0124	223	223	55
Constant load; step temperature																
7	2800	1537	2462	1350	6 000	41.37	3.74×10^{-12}	38	2.80×10^{-8}	380.9	1.11	------	0.0036	210	218	13
			2372	1300			------	--	1.29	286.5	.32	------	↓	↓	↓	↓
			2282	1250			------	--	.578	653.5	.31	------	↓	↓	↓	↓
24	3000	1648	2462	1350			3.00	21	3.93	333.7	1.05	.0034	.0037	217	177	3
			2372	1300			------	--	1.53	285.3	.41	------	↓	↓	↓	↓
			2282	1250			------	--	.649	670.0	.37	------	↓	↓	↓	↓
10	3200	1759	2462	1350			.243	27	1.40	1001.6	1.29	.0044	.0051	160	207	17
			2372	1300			------	--	.706	552.0	.43	------	↓	↓	↓	↓
			2282	1250			------	--	.294	855.0	.20	------	↓	↓	↓	↓
25	3600	1982	2462	1350			------	--	.668	2004.6	1.12	.0198	.0237	193	206	56
			2372	1300			------	--	.366	791.3	.28	------	↓	↓	↓	↓
			2282	1250	↓	↓	------	--	.138	3240.6	.36	------	↓	↓	↓	↓
28	3600	1982	2462	1350	8 000	55.16	------	--	1.61	1219.6	1.87	------	.0126	161	198	53
			2372	1300	↓	↓	------	--	.738	1368.5	1.24	------	↓	↓	↓	↓
			2282	1250	↓	↓	------	--	.219	839.2	.15	------	↓	↓	↓	↓
15	2800	1537	2372	1300	6 000	41.37	9.10	57	2.89	354.0	1.07	.0027	.0026	197	174	2
			2372	1300	7 000	48.26	------	--	3.62	167.0	.75	------				
			2372	1300	8 000	55.16	------	--	4.71	77.0	.60	------				
			2330	1275	↓	↓	------	--	3.22	66.0	.31	------				
			2282	1250	↓	↓	------	--	2.22	77.0	.24	------	↓	↓	↓	↓
Constant temperature; step load																
23	2800	1537	2372	1300	6 000	41.37	10.1×10^{-12}	69	2.64×10^{-8}	357.4	1.02	0.0027	0.0031	217	211	191
			↓	↓	7 000	48.26	------	--	3.05	168.5	.62	------	↓	↓	↓	↓
					8 000	55.16	------	--	3.34	335.0	1.70	------	↓	↓	↓	↓
17	3000	1648			6 000	41.37	2.48	59	1.82	620.0	1.15	.0034	.0038	185	171	27
					7 000	48.26	------	--	2.30	191.0	.61	------	↓	↓	↓	↓
			↓	↓	8 000	55.16	------	--	3.10	190.0	1.03	------	↓	↓	↓	↓
			2282	1250	8 000	55.16	------	--	1.55	122.0	.28	------	↓	↓	↓	↓
19	3200	1759	2372	1300	6 000	41.37	.137	70	.618	1845.0	1.03	.0044	.0053	157	193	25
			↓	↓	7 000	48.26	------	--	.856	843.0	1.03	------	↓	↓	↓	↓
					8 000	55.16	------	--	1.16	360	.62	------	↓	↓	↓	↓
21	3600	1982			6 000	41.37	1.58	--	-----	1606.5	.52	------	.0284	187	221	129
			↓	↓	7 000	48.26	------	--	.382	744.0	.25	------	↓	↓	↓	↓
					8 000	55.16	------	--	.564	625.0	.44	------	↓	↓	↓	↓

[a]All specimens were exposed 1 hr at indicated temperatures; variations in grain diameter are believed due to heating rate which was regulated by level of vacuum and degree of specimen outgassing.

Stress and Structure Dependency

The stress dependency of the secondary creep rate constant $\dot{\beta}$ was investigated for a series of step-load tests at 2372° F (1300° C). The results are shown in figure 6. It can be noted from this plot that the apparent exponential stress dependency n is not constant but varies with grain size. The fine-grained materials have apparent stress dependencies of 1.69 to 1.84 while the coarsest-grained material, which is also the most creep resistant under these conditions, has an apparent stress dependency of 2.92 over this narrow stress range. The variation of n with grain size is shown in figure 7.

The effect of grain size on the secondary creep rate constant $\dot{\beta}$ at constant stress is shown in figure 8. The creep rate decreases with increasing grain size rather sharply at fine-grain sizes but more slowly at larger grain sizes. This behavior is similar to that exhibited by Monel at 1100° and 1300° F (593° and 704° C) (ref. 12) and is consistent with creep deformation by a grain boundary sliding mechanism (ref. 13).

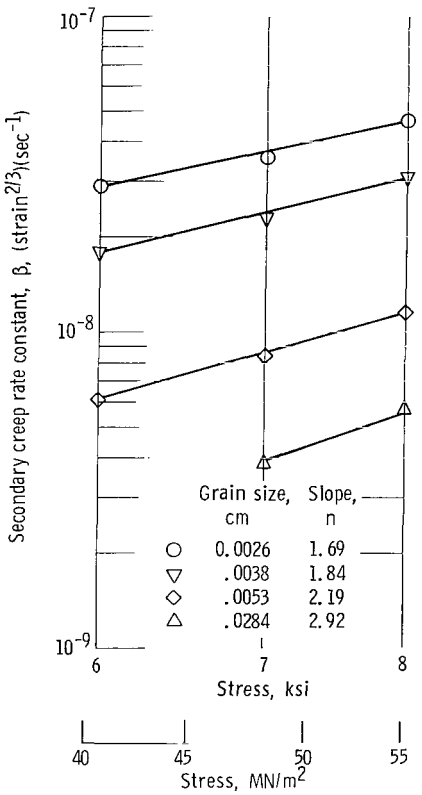

Figure 6. - Dependence of secondary creep rate constant on applied stress. Note that the slope (stress dependency) increases with increasing grain size.

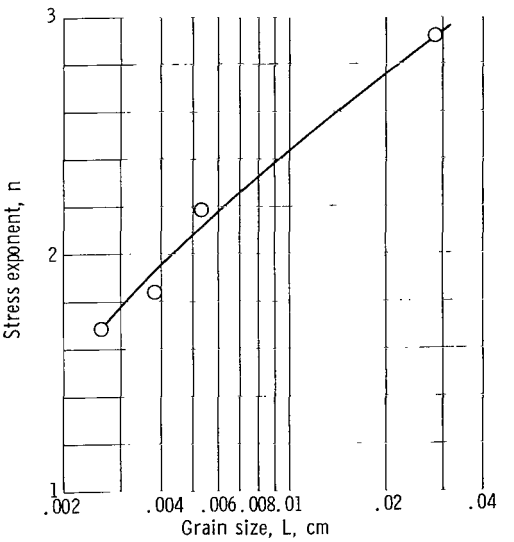

Figure 7. - Variation of stress exponent with grain size for creep tests on Ta-10W conducted at 2372° F (1300° C).

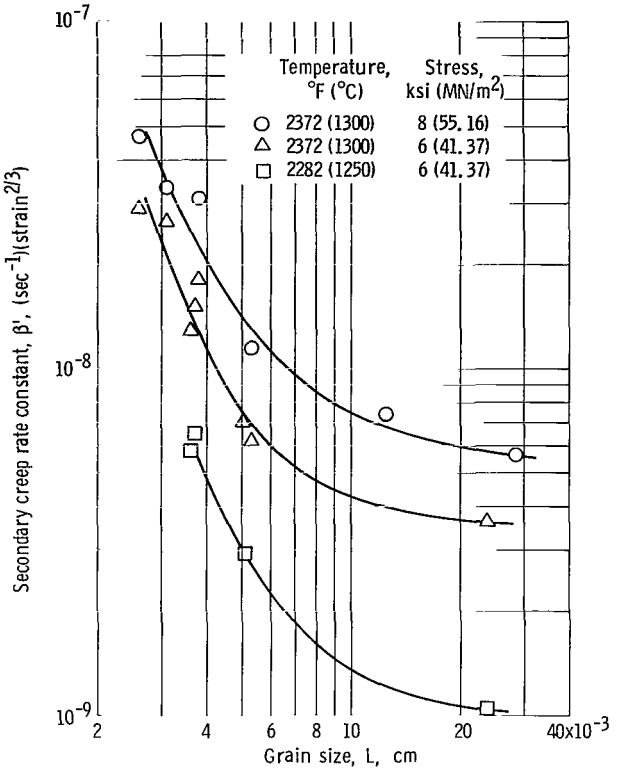

Figure 8. - Effect of grain size on secondary creep rate constant.

In order to relate the creep rate to both stress and structure, the concept of a structure-dependent effective stress was explored. This relation is expressed as

$$\sigma_e = \sigma_a + f(L) \tag{7}$$

and is similar to the familiar Petch relation with σ_e equal to the Petch σ_o but with the structural term added to rather than subtracted from the applied stress to give the effective stress.

The proper function of grain size was determined by first interpolating and extrapolating the creep data at 2282°, 2372°, and 2462° F (1250°, 1300°, and 1350° C) to give the creep strength at various grain sizes at a constant creep rate in the midrange of each set of data. Values of n for these calculations were taken from the curve in figure 7. These calculated strength values were then plotted against $L^{-1/2}$, L^{-1}, and L^{-2}. Figure 9 shows these plots for the data at 2372° F (1300° C). These plots indicate that for the majority of these data, the best fit is obtained for creep strength against L^{-2}.

The relation between effective stress and grain size was further investigated by

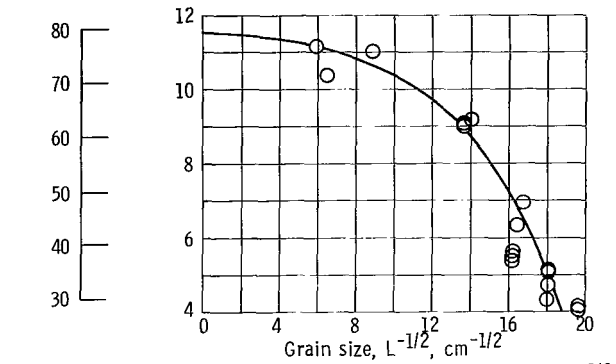

(a) Creep strength as function of (grain size)$^{-1/2}$.

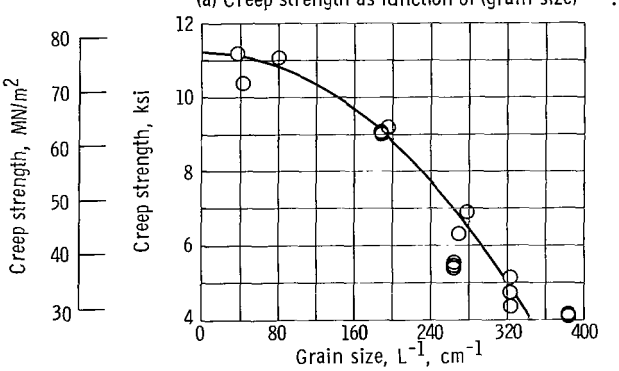

(b) Creep strength as function of (grain size)$^{-1}$.

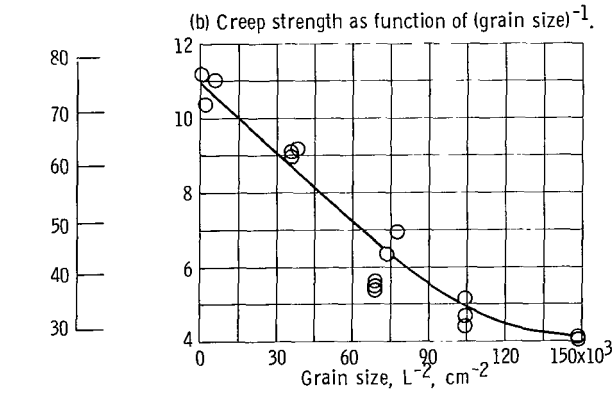

(c) Creep strength as function of (grain size)$^{-2}$.

Figure 9. - Relations between creep strength and grain size at 2372° F (1300° C) for a secondary creep rate constant of 1.5×10^{-8} second^{-1}.

least squares fitting the experimental data at 2372° F (1300° C) to power functions involving both L^{-1} and L^{-2} as follows:

$$\dot{\beta} = k_1\left(\sigma_a + \frac{A_1}{L}\right)^{n_1} \tag{8}$$

$$\dot{\beta} = k_2\left(\sigma_a + \frac{A_2}{L^2}\right)^{n_2} \tag{9}$$

The creep rates obtained from these relations are compared with the experimental data for stresses of 6 and 8 ksi (41.37 and 55.16 MN/m^2) in figure 10. Relation (9) is seen to fit these data somewhat better than relation (8). The better fit was confirmed by the correlation coefficients of the least-squares best fits, 0.963 for relation (8) and 0.971 for relation (9). Based on these analyses, relation (9) was used to relate structure, applied stress and secondary creep rate.

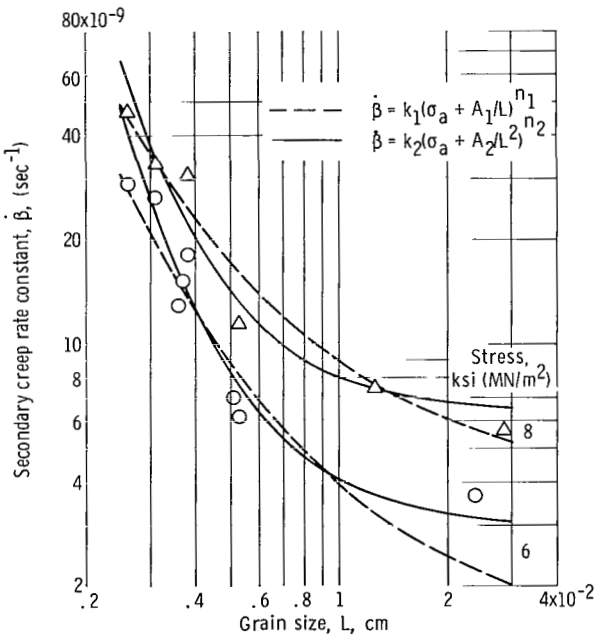

Figure 10. - Comparison of creep rate data at 2372° F (1300° C) with calculated rates assuming effective stress as function of L^{-1} and L^{-2}, respectively.

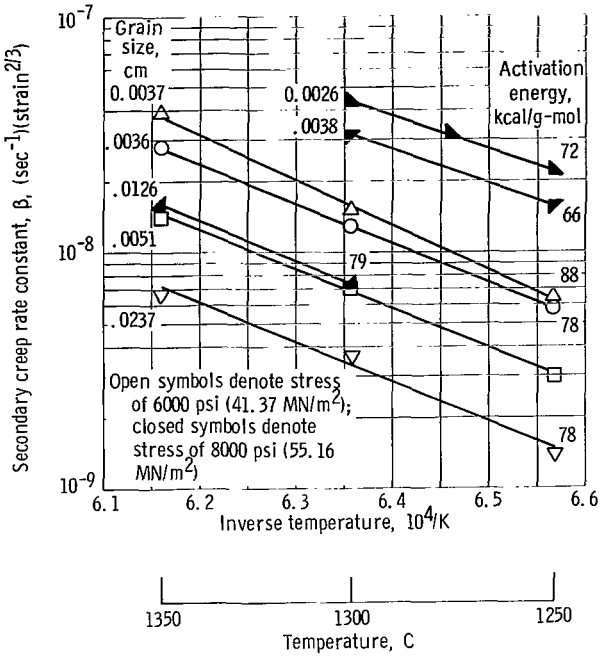

Figure 11. - Temperature dependency of secondary creep rate constants for various indicated grain sizes at 6000 and 800 psi (41.37 and 55.16 MN/m^2).

Temperature Dependency

An estimate of the temperature dependency of the secondary creep rate constant is provided by data from the step-temperature tests listed in table II. These data, plotted in figure 11, exhibit temperature dependencies corresponding to a rather wide range of activation energies (66 to 88 kcal/g-mole, with an average of 77 kcal/g-mole).

The activation energy was also determined by computer fitting all of the rate constant data to a relation of the form

$$\dot{\beta} = K\left(\sigma_a + \frac{A}{L^2}\right)^{n'} e^{-Q_c/RT} \tag{10}$$

This approach yielded an activation energy of 90.4 kilocalories per gram-mole, considerably higher than observed in the step-temperature tests. A plot of structure-compensated stress against temperature-compensated creep rate constant is shown in figure 12. The difference in apparent activation energies is attributed to the diffusion-controlled weakening reaction which also causes the accelerating creep curves. Since the extent of a diffusion-controlled reaction is normally proportional to temperature,

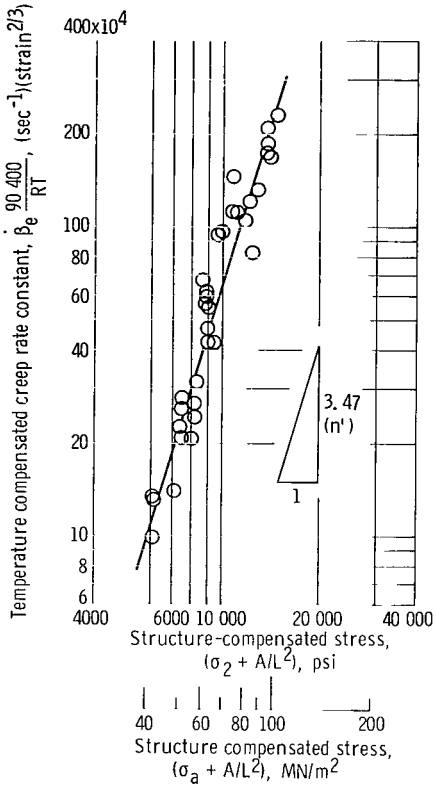

Figure 12. - Dependency of structure-compensated stress on the temperature-compensated secondary creep rate constant β'. This structure-compensated stress dependency is equal to 3.47.

the use of a decreasing step-temperature test, as employed in the present investigation, will cause the creep rate at a lower temperature to reflect the more rapid diffusion which occurred at the previous higher temperature. Since the diffusion reaction is weakening, the observed creep rates at lower temperatures in a step-temperature test will thus be more rapid than those observed in a constant temperature test, and, consequently, the apparent activation energy from such tests will be lower than from constant temperature tests. Thus, the difference in apparent activation energies reflects the nature of the step-temperature test employed and the activation energy determined from the overall correlation is more accurate.

Mechanism

The observation of increasing creep rate with decreasing grain size is consistent with the deformation mechanism commonly referred to as grain boundary sliding. How-

ever, the activation energy of 90.4 kilocalories per gram-mole is closer to that reported for lattice self-diffusion in tantalum (98.7 kcal/g-mole, ref. 14) than to that expected for boundary diffusion (about 0.5 of $Q_{lattice}$), again consistent with previous observation on the grain-boundary sliding. The actual mechanism is undoubtedly more complicated than the simple sliding of one grain relative to another, which might be expected to exhibit an activation energy similar to that for grain-boundary diffusion. It is more likely that grain-boundary sliding actually involves local deformation of the grain material adjacent to the boundary in order to accommodate sliding. This accommodation, occurring by dislocation climb, might be expected to be slower than the sliding process, occurring by grain-boundary diffusion, and hence, rate-limiting. Thus, we visualize creep deformation by grain-boundary sliding as one controlled by local dislocation climb in the vicinity of the grain boundary rather than one controlled by the sliding process itself.

The use of an effective stress related to the applied stress by a grain size term as expressed in equation (7) is similar although opposite in sign to the Petch relation, as pointed out earlier. The difference in sign results from the fact that grain boundaries are strengthening at low temperatures, where the Petch relation is applicable, while at higher temperatures where grain-boundary sliding is predominant, grain boundaries are weakening. The effective stress in equation (6) is theoretically that of a material of infinitely large grain size, that is, a large single crystal.

The proper grain size function of equation (7) is not clear from mechanistic considerations. The grain-boundary area per unit volume is proportional to L^2/L^3 or L^{-1}. This function has been suggested by Garofalo in his alternate expression (eq. (1)) for incorporating structure effects, and it is in contrast to the L^{-2} function derived empirically in the present study. The proper grain size may well depend on such factors as the thickness of the adjacent boundary region which deforms to accommodate grain-boundary sliding and/or solute segregation to or from this region.

The dependence of strain on time$^{3/2}$ was exhibited by all creep curves in the present study. The basis for this derivation from the normal second-stage linearity of strain-time curves is not associated with precipitation or agglomeration of a second phase since the material employed here was a clean, single-phase alloy. Neither does this behavior appear attributable to oxygen losses during high-vacuum exposure, as suggested by Sheffler et al. (ref. 6) for the Ta-8W-2Hf alloy, since analysis indicated slight increases in oxygen content in the present study (table II). It does appear probable that the time$^{3/2}$ dependency of creep strain is related to diffusion-controlled reaction which results in a weakening of the Ta-10W alloy. This suggestion is strengthened by the discrepancy in apparent activation energies for creep, with the decreasing step-temperature tests showing a lower apparent activation energy than that shown by the entire set of data, including primarily results at constant temperatures. This discrepancy, as dis-

cussed earlier, can be expected if a temperature-dependent diffusion reaction occurs during creep.

The nature of the diffusion-controlled reaction is not clear at this time. One possibility is depletion of tungsten from the vicinity of the grain boundaries, which could be expected to accompany vacancy annihilation at grain boundaries if the tungsten-vacancy binding energy is only weakly positive and if the mobility of tungsten is greater than that of tantalum (ref. 15). Unfortunately, compositional changes in the vicinity of the grain boundaries are difficult to detect in a concentrated alloy such as Ta-10W; neither microhardness traverses nor electron-probe studies of a specimen crept for 3018 hours at 2200° F (1204° C) could detect significant differences between the grain boundaries and the grain interiors.

CONCLUSIONS

The following conclusions are drawn from this study on the long-time creep behavior of Ta-10W in the 2000° to 2600° F (1093° to 1426° C) range:

1. Grain size exerts a significant effect on creep behavior, the creep strength decreasing with decreasing grain size. Creep rate can be related to applied stress σ_a and grain size L through the introduction of an effective stress σ_e:

$$\dot{\beta} = K\sigma_e^{n'} = K\left(\sigma_a + \frac{A}{L^2}\right)^{n'}$$

The predominant deformation mechanism is believed to be that commonly referred to as grain-boundary sliding, although the observed activation energy suggests that deformation by dislocation climb in regions adjacent to the grain boundaries in order to accommodate grain-boundary sliding may be rate controlling.

2. Creep strain during secondary creep is proportional to time$^{3/2}$. This is interpreted to result from a concurrent, diffusion-controlled reaction which weakens Ta-10W, possibly desegregation of tungsten from grain-boundary regions.

3. Second-stage creep of Ta-10W under the conditions of the present study can be described by

$$\frac{\epsilon^{2/3}}{t} = \dot{\beta} = K\left(\sigma_a + \frac{A}{L^2}\right)^{n'} e^{-Q_c/RT}$$

where

$\epsilon^{2/3}/t$	creep rate
σ_a	applied stress
L	grain size
T	temperature
K	8.35×10^{-10} sec^{-1} $(psi)^{-3.47}$
A	0.0389 psi $(cm)^2$
n'	3.47
Q_c	90 400 cal/g-mole
R	1.986 cal/g-mole

Lewis Research Center,
National Aeronautics and Space Administration,
Cleveland, Ohio, May 27, 1970,
129-03.

REFERENCES

1. Titran, Robert H.; and Hall, Robert W.: Ultrahigh-Vacuum Creep Behavior of Columbium and Tantalum Alloys at 2000° and 2200° F for Times Greater than 1000 Hours. Refractory Metals and Alloys IV - Research and Development. R. I. Jaffee, G. M. Ault, J. Maltz, and M. Semchyshen, eds., Gordon and Breach Science Publ., 1967, pp. 761-774.
2. Titran, Robert H.; and Hall, Robert W.: High-Temperature Creep Behavior of a Columbium Alloy, FS-85. NASA TN D-2885, 1965.
3. Titran, Robert H.: Creep of Tantalum T-222 Alloy in Ultrahigh Vacuum for Times up to 10 000 Hours. NASA TN D-4605, 1968.
4. McCoy, H. E.: Creep Properties of the Nb-1%Zr Alloy. J. Less Common Metals, vol. 8, no. 1, Jan. 1965, pp. 20-35.
5. Stephenson, R. L.: Creep-Rupture Properties of FS-85 Alloy and Their Response to Heat Treatment. Rep. ORNL-TM-1456, Oak Ridge National Lab., July 1966.

6. Sheffler, K. D.; Sawyer, J. C.; and Steigerwald, E. A.: Mechanical Behavior of Tantalum-Base T-111 Alloy at Elevated Temperatures. Trans. ASM, vol. 62, no. 3, 1969, pp. 749-758.

7. Garofalo, F.; Domis, W. F.; and von Gemmingen, F.: Effect of Grain Size on the Creep Behavior of an Austenitic Iron-Base Alloy. Trans. AIME, vol. 230, no. 6, Oct. 1964, pp. 1460-1467.

8. Lawley, A.; Coll, J. A.; and Cahn, R. W.: Influence of Crystallographic Order on Creep of Iron-Aluminum Solid Solutions. Trans. AIME, vol. 218, no. 1, Feb. 1960, pp, 166-177.

9. Howard, Eugenia M.; Barmore, Willis L.; Mote, Jim D.; and Dorn, John E.: On the Thermally-Activated Mechanism of Prismatic Slip in the Silver - Aluminum Hexagonal Intermediate Phase. Trans. AIME, vol. 227, no. 5, Oct. 1963, pp. 1061-1068.

10. Hall, R. W.; and Titran, R. H.: Creep Properties of Columbium Alloys in Very High Vacuum. Refractory Metals and Alloys III: Applied Aspects. R. I. Jaffee, ed., Gordon and Breach Science Publ., Inc., 1966, pp. 885-900.

11. Crussard, C.: Thirty Years of Dislocation Theory and of Rheology - A Study of Transient Creep. ASM Trans. Quarterly, vol. 57, no. 4, Dec. 1964, pp. 778-803.

12. Shahinian, Paul; and Lane, Joseph R.: Influence of Grain Size on High Temperature Properties of Monel. Trans. ASM, vol. 45, 1953, pp. 177-199.

13. Garofalo, Frank: Fundamentals of Creep and Creep-Rupture in Metals. Macmillian Co., 1965, pp. 127-155.

14. Pawel, R. E.; and Lundy, T. S.: The Diffusion of Nb^{95} and Ta^{182} in Tantalum. J. Phys. Chem. Solids, vol. 26, 1965, pp. 937-942.

15. Hanneman, R. E.; and Anthony, T. R.: Effects of Non-Equilibrium Segregation on Near-Surface Diffusion. Acta Met, vol. 17, no. 9, Sept. 1969, pp. 1133-1140.

NASA-Langley, 1970 —— 17 E-5389

NATIONAL AERONAUTICS AND SPACE ADMINISTRATION
WASHINGTON, D. C. 20546
OFFICIAL BUSINESS

FIRST CLASS MAIL

POSTAGE AND FEES PAID
NATIONAL AERONAUTICS AND
SPACE ADMINISTRATION

"The aeronautical and space activities of the United States shall be conducted so as to contribute . . . to the expansion of human knowledge of phenomena in the atmosphere and space. The Administration shall provide for the widest practicable and appropriate dissemination of information concerning its activities and the results thereof."

—NATIONAL AERONAUTICS AND SPACE ACT OF 1958

NASA SCIENTIFIC AND TECHNICAL PUBLICATIONS

TECHNICAL REPORTS: Scientific and technical information considered important, complete, and a lasting contribution to existing knowledge.

TECHNICAL NOTES: Information less broad in scope but nevertheless of importance as a contribution to existing knowledge.

TECHNICAL MEMORANDUMS: Information receiving limited distribution because of preliminary data, security classification, or other reasons.

CONTRACTOR REPORTS: Scientific and technical information generated under a NASA contract or grant and considered an important contribution to existing knowledge.

TECHNICAL TRANSLATIONS: Information published in a foreign language considered to merit NASA distribution in English.

SPECIAL PUBLICATIONS: Information derived from or of value to NASA activities. Publications include conference proceedings, monographs, data compilations, handbooks, sourcebooks, and special bibliographies.

TECHNOLOGY UTILIZATION PUBLICATIONS: Information on technology used by NASA that may be of particular interest in commercial and other non-aerospace applications. Publications include Tech Briefs, Technology Utilization Reports and Notes, and Technology Surveys.

Details on the availability of these publications may be obtained from:

SCIENTIFIC AND TECHNICAL INFORMATION DIVISION

NATIONAL AERONAUTICS AND SPACE ADMINISTRATION

Washington, D.C. 20546